Attribution of aerosol particle number size distributions to major sources using a 11-year-long urban dataset

Máté Vörösmarty[1], Philip K. Hopke[2,3], and Imre Salma[4]

[1] Hevesy György Ph.D. School of Chemistry, Eötvös Loránd University, Budapest, Hungary
[2] Department of Public Health Sciences, University of Rochester School of Medicine and Dentistry, Rochester, NY, USA
[3] Institute for a Sustainable Environment, Clarkson University, Potsdam, NY, USA
[4] Institute of Chemistry, Eötvös Loránd University, Budapest, Hungary

Correspondence: Imre Salma (salma.imre@ttk.elte.hu) and Máté Vörösmarty (vmate6@student.elte.hu)

Table S1. Start and end dates of the measurement years with the median concentrations of total particle numbers ($N_{6–1000}$; in 10^3 cm^{-3}), NO, NO_2, O_3, CO, SO_2 and PM_{10} mass (all in μg m^{-3}). The measurements in year Y2 were conducted in the near-city background, whereas the other data were obtained in the urban background of Budapest.

Year	Start	End	$N_{6–1000}$	NO	NO_2	O_3	CO	SO_2	PM_{10}
Y1	3–Nov–2008	2–Nov–2009	11.3	13.4	37	25	547	5.0	33
Y2	19–Jan–2012	18–Jan–2013	4.2	3.9	15.4	51	378	6.1	23
Y3	13–Nov–2013	12–Nov–2014	9.8	19.7	47	18.3	489	4.8	31
Y4	13–Nov–2014	12–Nov–2015	9.4	23	48	20	577	4.6	39
Y5	13–Nov–2015	12–Nov–2016	7.6	17.7	42	25	513	4.8	29
Y6	28–Jan–2017	27–Jan–2018	10.6	20	44	21	534	4.5	28
Y7	28–Jan–2018	27–Jan–2019	10.3	17.2	43	21	669	5.2	36
Y8	28–Jan–2019	27–Jan–2020	10.7	26	42	20	625	4.9	34
Y9	28–Jan–2020	27–Jan–2021	8.6	10.8	33	25	526	5.0	26
Y10	28–Jan–2021	27–Jan–2022	9.6	12.9	36	28	589	4.5	25
Y11	28–Jan–2022	28–Jan–2023	9.0	10.5	31	35	607	5.2	22

Table S2. Seasonal means ± standard deviations of the air temperature (*T*, in °C), relative humidity (RH, in %), wind speed above the rooftop level (WS, in m s^{-1}) and global radiation for individual values > 10 W m^{-2} (GRad, in W m^{-2}) over the investigated years.

Parameter	spring	summer	autumn	winter
T	13.1±6.4	23.4±4.9	13.0±6.4	2.9±4.4
RH	60±19	59±18	75±20	80±16
WS	3.0±1.9	2.7±1.6	2.4±1.6	2.8±1.9
GRad	375±211	442±257	261±145	163±83

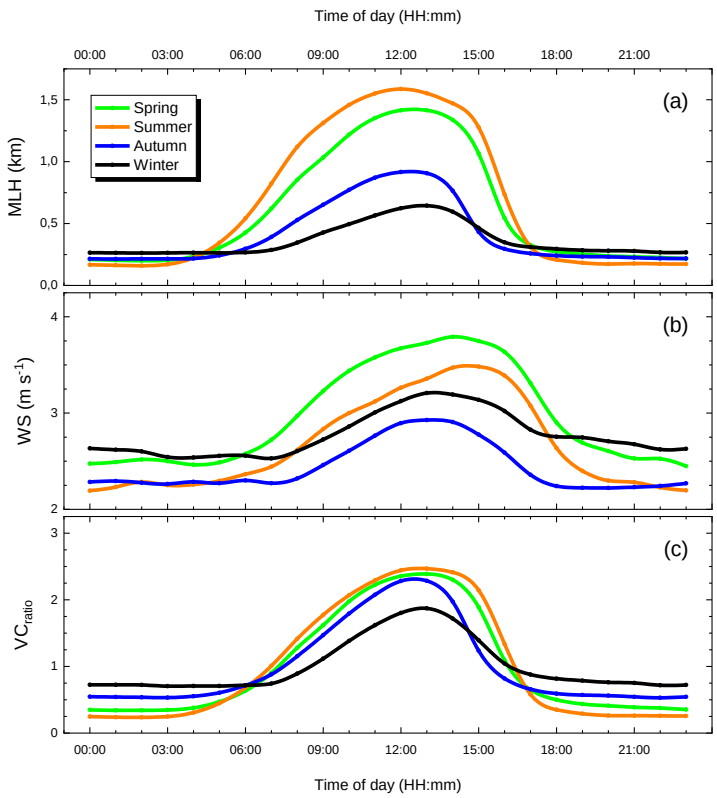

Figure S1. Mean diel variation of the planetary boundary mixing layer height (MLH; a), wind speed (WS; b) and ventilation coefficient ratio (VC_{ratio}; c) separately for spring, summer, autumn and winter.

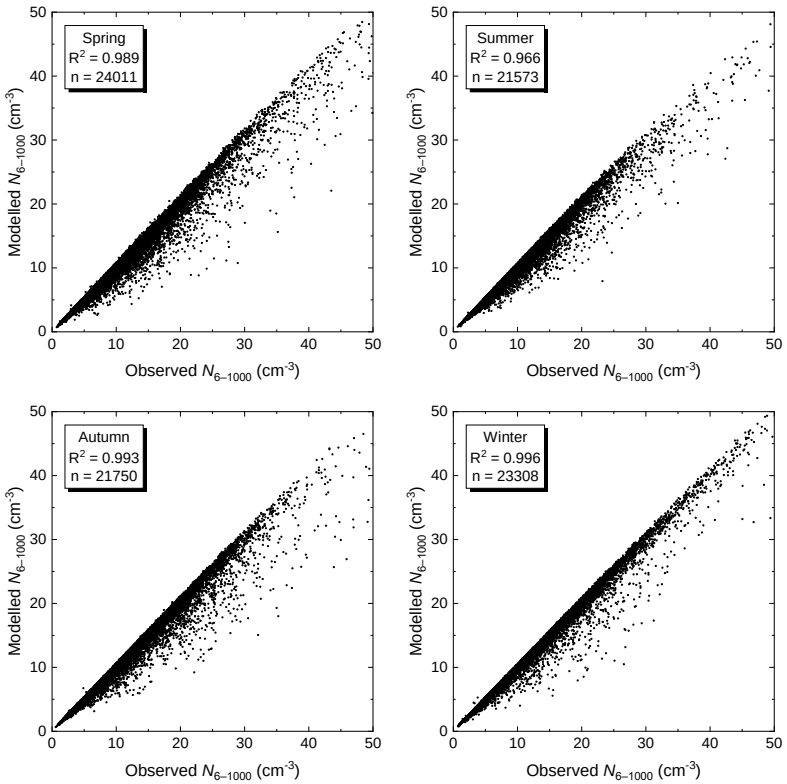

Figure S2. Scatter plots of the modelled (by uncorrected PMF approach) and measured total particle number concentrations ($N_{6–1000}$) for spring, summer, autumn and winter. The coefficient of determination (R^2) and total number of observations (n) are also indicated.

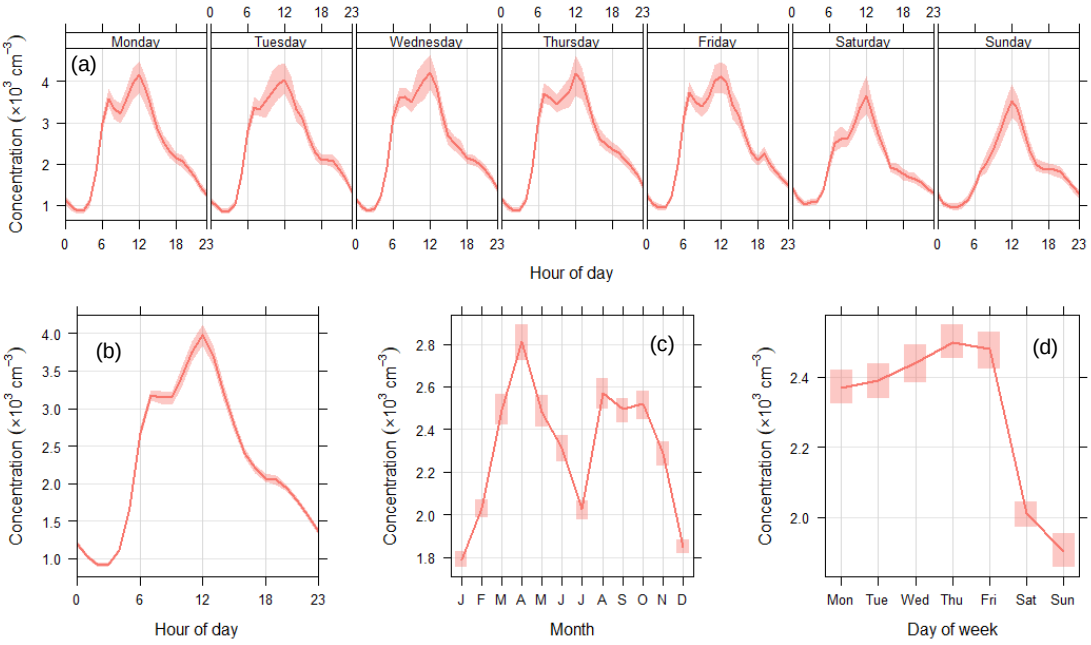

Figure S3. Mean variations of the total particle number concentration associated with the nucleation source as diel time series for day of week (a), for all days (b), as monthly means for month of year (c) and as daily means for day of week (d). The coloured bands around the lines indicate 95 % confidence interval of the mean.

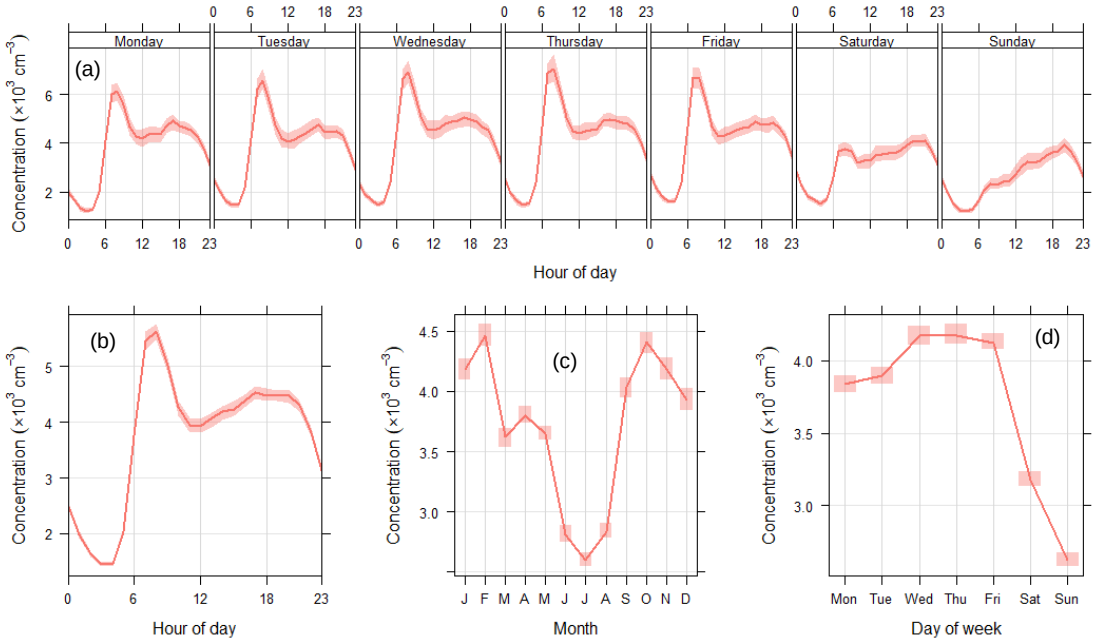

Figure S4. Mean variations of the total particle number concentration associated with the vehicle traffic semi-volatile fraction as diel time series for day of week (a), for all days (b), as monthly means for month of year (c) and as daily means for day of week (d). The coloured bands around the lines indicate 95 % confidence interval of the mean.

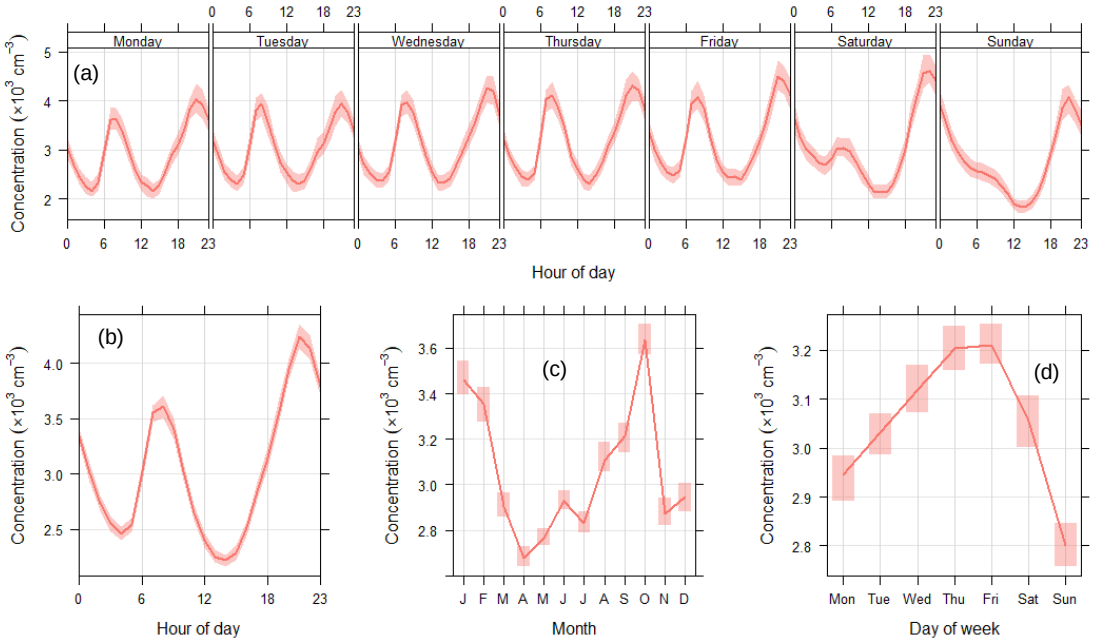

Figure S5. Mean variations of the total particle number concentration associated with vehicle traffic solid fraction as diel time series for day of week (a), for all days (b), as monthly means for month of year (c) and as daily means for day of week (d). The coloured bands around the lines indicate 95 % confidence interval of the mean.

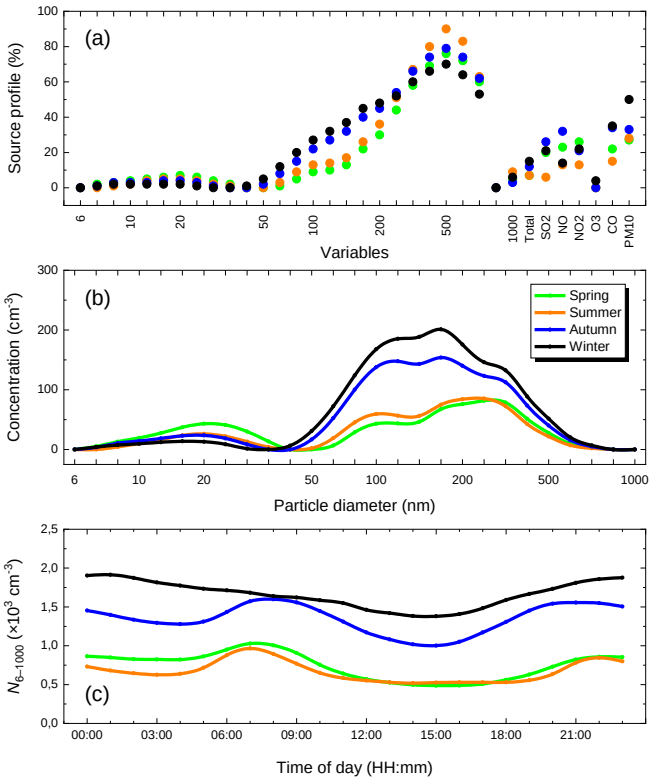

Figure S6. Relative factor profile (a), factor contribution to the particle number concentrations in the size channels (b), and the mean diel variation of the total particle number ($N_{6–1000}$; c) assigned to the urban diffuse source for spring, summer, autumn and winter. The exact diameters of the size channels are listed in Sect. 2.1.

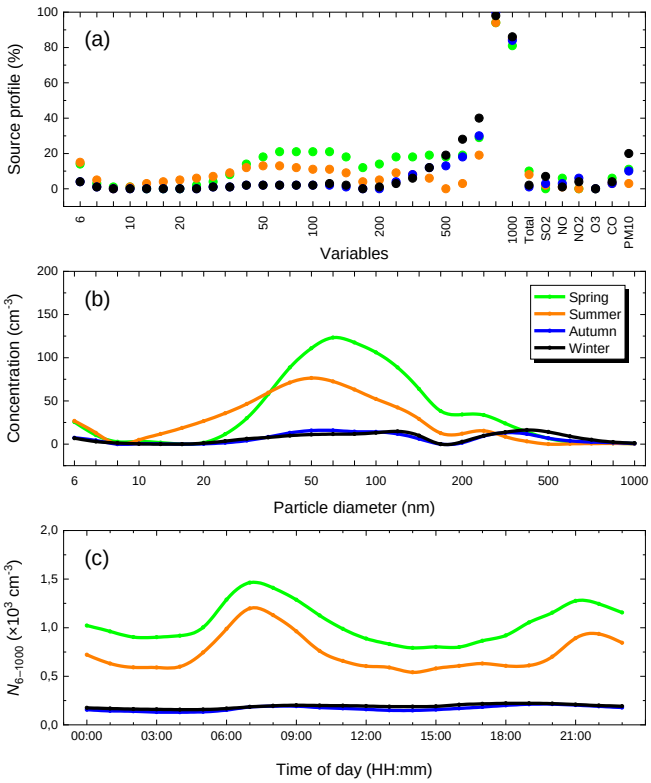

Figure S7. Relative factor profile (a), factor contribution to the particle number concentrations in the size channels (b), and the mean diel variation of the total particle number ($N_{6–1000}$; c) assigned to the source of secondary inorganic aerosol for spring, summer, autumn and winter. The exact diameters of the size channels are listed in Sect. 2.1.

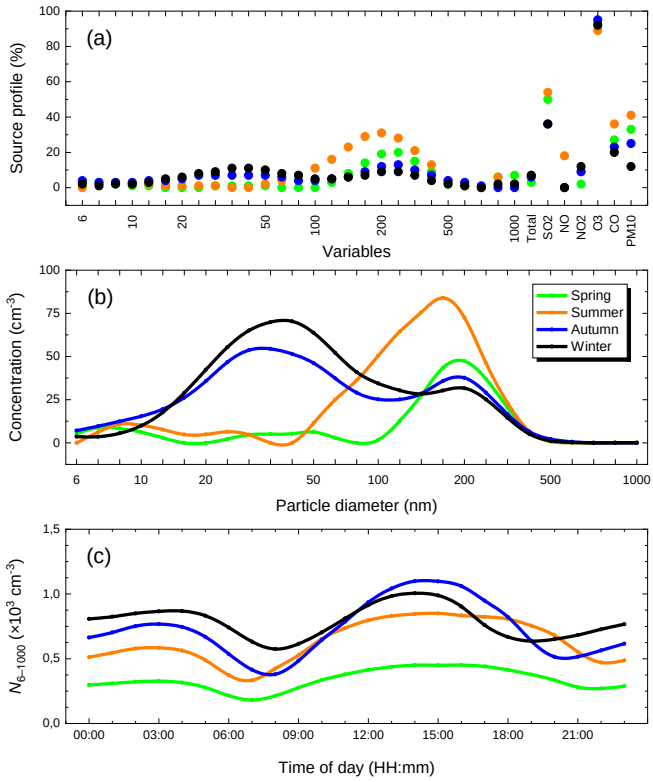

Figure S8. Relative factor profile (a), factor contribution to the particle number concentrations in the size channels (b), and the mean diel variation of the total particle number ($N_{6–1000}$; c) assigned to the source of O_3-associated secondary aerosol for spring, summer, autumn and winter. The exact diameters of the size channels are listed in Sect. 2.1.

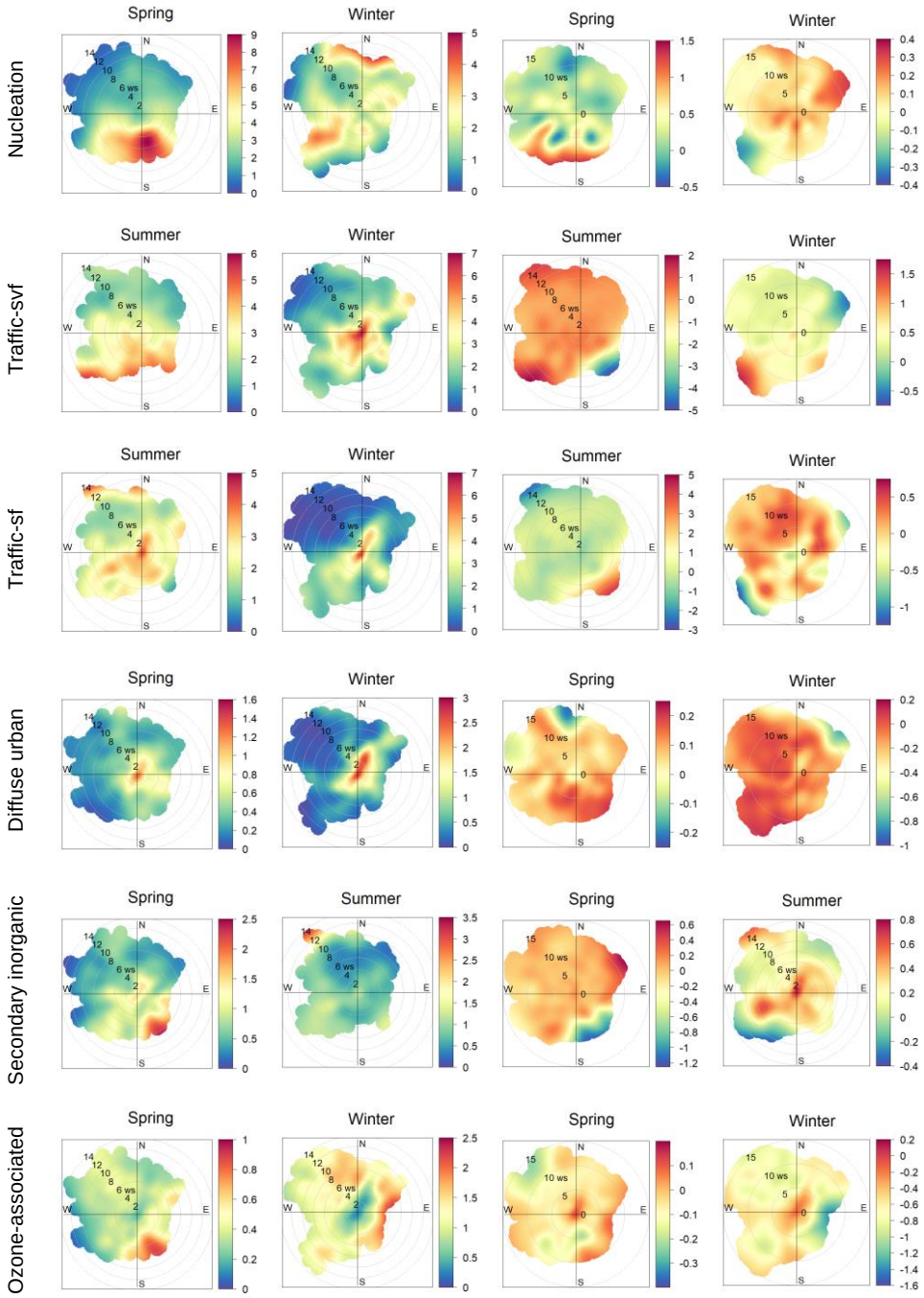

Figure S9. Conditional bivariate probability plots of the contributions from nucleation, traffic semi-volatile fraction (traffic-svf), traffic solid fraction (traffic-sf), diffuse urban, secondary inorganic aerosol and ozone-associated secondary aerosol sources derived by uncorrected PMF approach to the total particle number concentration ($N_{6–1000}$; in 10^3 cm^{-3}; first and second columns from left), and the (DC-PMF – uncorrected PMF) difference for the $N_{6–1000}$ (in 10^3 cm^{-3}; third and fourth columns from left) in selected season pairs. The values of WS are given in m s^{-1}. Note the different scales of the colour bar.